Multiparty entanglement routing in quantum networks

Vaisakh Mannalath [*]
Department of Physics and Materials Science & Engineering, Jaypee Institute of Information Technology, A-10, Sector 62, Noida, UP-201309, India;
Vigo Quantum Communication Center, University of Vigo, Vigo E-36310, Spain;
Escuela de Ingeniería de Telecomunicación, Department of Signal Theory and Communications, University of Vigo, Vigo E-36310, Spain;
and AtlanTTic Research Center, University of Vigo, Vigo E-36310, Spain

Anirban Pathak [†]
Department of Physics and Materials Science & Engineering, Jaypee Institute of Information Technology, A-10, Sector 62, Noida, UP-201309, India

(Received 11 February 2023; accepted 1 December 2023; published 19 December 2023)

Distributing entanglement among multiple users is a fundamental problem in quantum networks, requiring an efficient solution. In this work, a protocol is proposed for extracting maximally entangled ($|\mathrm{GHZ}_n\rangle$) states for any number of parties in a quantum network. It is based on the graph-state formalism and requires minimal assumptions on the network state. The protocol only requires local measurements at the network nodes and just a single-qubit memory per user. Existing protocols on bipartite entanglement routing are also improved for specific nearest-neighbor network architectures. To this end, the concept of majorization is utilized to establish a hierarchy among different paths in a network based on their efficacy. This approach utilizes the symmetry of the underlying graph state to obtain better-performing algorithms.

DOI: 10.1103/PhysRevA.108.062614

I. INTRODUCTION

Point-to-point secure quantum communication has been achieved quite successfully with optical fibers [1] and in free space, [2]. However, direct quantum communication is limited by errors and losses incurred during transmission [3]. To overcome these inherent limitations and to establish connections over long distances, approaches based on entanglement swapping are employed [4,5]. Over recent years, a set of such protocols have been experimentally implemented with increasing distances and success rates [6–8]. In fact, with the help of a satellite, intercontinental quantum communication has already been performed between China and Austria [9]. Apart from pushing the boundaries of what is possible regarding maximum distance [10] and communication rates [11], a natural step forward would be to consider multiparty scenarios. Naturally, the community hopes to develop more complicated networks involving multiple nodes leading to a quantum internet [12]. A fundamental requirement for realizing a quantum internet is to develop algorithms for managing the entanglement present in the network and, thus, to distribute entangled states among two or more specific nodes (users) [13–16]. This easy-to-state algorithm designing problem is fundamental and challenging, and under the chosen condition, it leads to a set of related problems of interest. Assuming that the future quantum network architectures might only allow for nearest-neighbor interactions, it might not be feasible to directly distribute quantum states between distant users. Nevertheless, such short-range interactions could be used to establish some multipartite state among the entire user network from which the useful states would have to be then extracted, using local operations within the nodes and classical communication among the nodes. Nodes could also be assumed to have limited capabilities in applying arbitrary operations on qubits. In general, it is not easy to determine if a state can be transformed to another with a restricted operation or measurement set. For example, in Ref. [17], the authors investigated whether a given multipartite state can be transformed into a set of Bell states between specific network nodes using operations restricted to single-qubit Clifford operations, single-qubit Pauli measurements, and classical communication. They showed that this specific problem is NP-complete. This result highlights the difficulty of the problem at hand and the crucial need to devise better-performing protocols, at least for some specific instances relevant to multipartite schemes. Motivated by the importance and hardness of this problem, here we aim to revisit the task in a more general scenario. Specifically, we wish to devise an efficient scheme for transforming a given network state into a multipartite Greenberger-Horne-Zeilinger (GHZ) state among the specific nodes of the network using operations restricted to single-qubit Pauli measurements.

Before we proceed further, it would be apt to note that the effectiveness of quantum networks in performing tasks that are unachievable in the classical world (in classical networks) is not restricted to secure quantum communication only. Many protocols in the multiparty scenario have been proposed for tasks like quantum secret sharing [18–21], quantum voting

*vaisakhmannalath@gmail.com
†anirban.pathak@jiit.ac.in

[22–24], and quantum conference key agreement [25–28], utilizing shared GHZ states. The study of such quantum network protocols is an active field with promising applications. Quantum networks are also helpful in distributed quantum computing [29,30], clock synchronization [31–34], and many other applications. Most of these applications require the ability to distribute entanglement among two or more network nodes located far away. Motivated by this, a few schemes for generating entanglement among specific network nodes have been proposed in the recent past [35–38], and some of them have been implemented experimentally [39–42]. Interestingly, the optimal or maximally efficient protocol for remote entanglement generation in a quantum network has yet to be discovered. This motivated us to look at the possibility of designing a more efficient algorithm for the entanglement distribution among the nodes of a network.

A helpful tool used in the study of quantum networks is the notion of graph states [43,44]. They have been employed to realize several tasks in quantum information processing, including quantum metrology [45], quantum error-correcting codes [46], and one-way quantum computing [47]. Furthermore, a strong interplay between the graph theory and quantum entanglement is known, and the same has been investigated from various perspectives [44,48,49]. Graph states can be generated in a network when the nodes, sharing maximally entangled pairs with nearby nodes, perform suitable entanglement-generating operations locally. Alternatively, a graph state could be prepared at one node and subsequently the qubits may be distributed with the other nodes of the network in a manner that each node receives a qubit. Graph states have been studied extensively in the context of quantum networks [50,51], with much of the research focused on generating them in a quantum network with varying assumptions [14,52–54].

A general method for extracting maximally entangled states with two or three parties in connected networks was presented in Ref. [53]. They consider manipulating an already generated graph state to accommodate future communication requests. Compared to other methods, such as the algorithm described in Ref. [55], which requires large amounts of quantum memories, this approach was more advantageous regarding the memory required for the repeater stations. In the graph-state formalism, the maximally entangled states shared by two (three) parties are represented by line graphs, with two (three) vertices, up to some local operations. Hence, to establish a maximally entangled state between two (three) nodes, we could perform a sequential entanglement swapping protocol on a path connecting all two (three) nodes. The protocol proposed in Ref. [53] is quite similar to such repeater-based protocols, albeit more efficient. However, this simple approach will not work for four or more nodes since the corresponding graphs are not line graphs [44]. Moreover, two nodes, in general, can be connected by a number of different paths; the protocol in Ref. [53] does not provide a way to evaluate these different possibilities and pick the right one.

In our work, we define a protocol for extracting maximally entangled states for any number of parties. The protocol only requires local measurements performed by the network users with access to a single-qubit memory. To achieve this, we extensively use graph-theoretic tools in the graph-state formalism of quantum networks. Our protocol can be viewed as a generalization of the results in Ref. [53], where a criterion was laid out for the extraction of four partite GHZ states. We improve upon their results and provide a criterion that works for n-partite GHZ states. Moreover, we improve upon the results of the authors of Ref. [53] by providing a more efficient routine for establishing connections between two distant nodes of a network. We use the concept of majorization [56] to establish a hierarchy among different paths in a network based on their efficiency. This concept utilizes the symmetry of the underlying graph state to obtain better-performing algorithms.

The rest of the paper is organized as follows. In Sec. II, we briefly introduce graph states and the graph theory tools that we use. Then, in Sec. III, we state and prove the theorem concerning multipartite state generation and demonstrate several examples. In Sec. IV, we consider a class of nearest neighbor graphs and improve upon the existing entanglement routing protocols for those specific cases. In Sec. V we conclude with our remarks and possible future research questions.

II. PRELIMINARIES

An undirected finite graph $G = (V, E)$ is defined by a set of vertices $V \subsetneq \mathbb{N}$ and a set $E \subseteq V \times V$ of edges. A simple graph is a graph without any loop (an edge that connects a vertex with itself) and without multiple edges connecting the same pair of vertices. The set of all vertices having a shared edge with a given vertex a is called the neighborhood of a and is denoted by N_a.

Definition II.1. (Vertex Deletion): Deleting a vertex v results in a graph where the vertex v and all the edges connected to it are removed

$$G - v = (V \backslash v, \{e \in E : e \cap v = \varnothing\}).$$

.

Definition II.2. (Local complementation): A local complementation LC_v is a graph operation specified by a vertex v, taking a graph G to $LC_v(G)$ by replacing the neighborhood of v by its complement

$$LC_v(G) = (V, E \Delta K_{N_v}),$$

where K_{N_v} is the set of edges of the complete graph on the vertex set N_v and $E \Delta K_{N_v} = (E \cup K_{N_v}) - (E \cap K_{N_v})$ is the symmetric difference.

Local complementation acts on the neighborhood of a vertex by removing edges if they are present and adding missing edges, if any.

Definition II.3. (Vertex-minor): A graph H is called a vertex-minor of G if a sequence of local complementations and vertex-deletions maps G to H.

The simple graph G defined so far is a mathematical entity, but in the quantum world, we can associate a pure quantum state $|G\rangle$ with it, called a graph state. A graph state is defined on a Hilbert space $\mathcal{H}_V = (\mathbb{C}^2)^{\otimes V}$. Specifically, each vertex in V is assigned a qubit in the state $|+\rangle = (|0\rangle + |1\rangle)/\sqrt{2}$. Subsequently, a controlled-Z operation is applied to a pair of qubits sharing an edge to construct the graph state $|G\rangle$ associated with the graph G [44]. Thus, a graph state is defined as follows:

$$|G\rangle := \prod_{(i,j)\in E} CZ_{i,j}|+\rangle^{\otimes V}.$$

Local Clifford operations on graph states defined above can be represented using local complementations on the corresponding graph [57]. Local Pauli measurements on the graph states can be represented using local complementations and vertex deletions [44]. We can visualize the role played by the Pauli measurements as follows.

Proposition 1. (Z measurement): Measurement of a qubit, corresponding to the vertex v, in the Z basis is represented by the vertex deletion of v,

$$Z_v(G) = G - v.$$

Proposition 2. (Y measurement): Measurement of a qubit, corresponding to the vertex v, in the Y basis is represented by

$$Y_v(G) = Z_v LC_v(G).$$

Proposition 3. (X measurement): Measurement of a qubit, corresponding to the vertex v, in the X basis is represented by

$$X_v(G) = LC_w Z_v LC_v LC_w(G),$$

where $w \in N_v$.

Note that the state represented by the graph obtained under the application of Pauli measurement transformations defined above and the actual state are only equivalent under some local Clifford rotations (Sec. III [44]). We omit this distinction for the rest of the paper.

Definition II.4. (Repeater Line): A path for which $E(V, V) = \{(v_1, v_2), \ldots, (v_{n-1}, v_n)\}$ for $V = \{v_1, \ldots, v_n\}$ is called a repeater line.

Definition II.5. (Neighborhood): The set of all vertices sharing an edge with vertex v, is called the neighborhood of v. Neighborhood of a path is defined as the union of neighborhoods of all vertices in the path.

III. GHZ STATES

We already stated a set of definitions and propositions which allow us to initiate the discussion on the solution of a problem stated as follows: Given a graph state, how can we efficiently share entangled states between multiple parties that are not connected via physical channels? To answer this question, let us first look at the simplest example of connecting two distant nodes through a shared Bell pair. The straightforward solution would be to find the shortest path connecting the two nodes with the smallest combined neighborhood, performing Z measurements on the nodes that do not lie on the path and sequential X measurement on all the intermediate nodes on the path [see Figs. 1(a) to 1(c) for an illustrative example]. Here, the initial Z measurements would isolate a repeater line between the initial vertices, and the X measurement on a vertex has the simple action of connecting its neighbours and deleting the vertex itself. It is easy to see then how this protocol gives the desired result. Since a $|\mathrm{GHZ}_3\rangle$ state can also be represented using a line graph, the same protocol as above can also be applied there. First, we find a path connecting all three nodes between which the $|\mathrm{GHZ}_3\rangle$ state is to be distributed, isolate it from the rest of the graph using

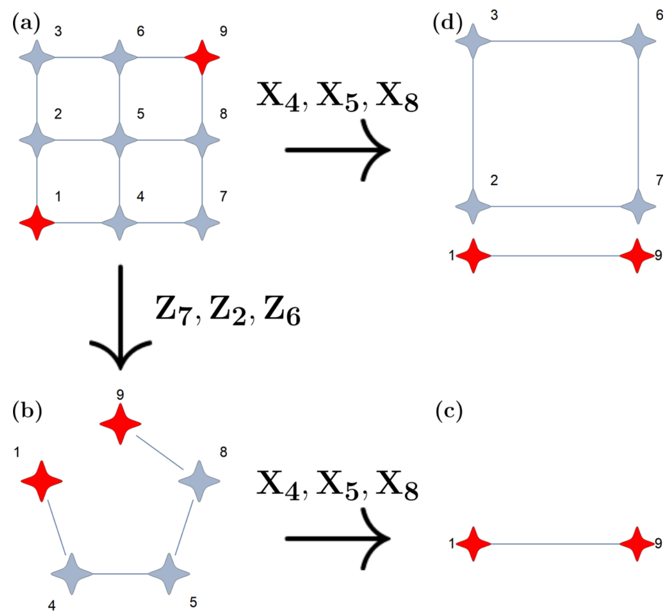

FIG. 1. Repeater protocol and X protocol [53] (a) 3×3 square grid. The objective is to establish a Bell pair between the vertices 1,9. (b), (c) Repeater protocol. First, we isolate a repeater line 1,4,5,8,9 with Z measurements on the neighborhood vertices 7,2,6. Then intermediate vertices along the repeater line are measured in the X basis sequentially, resulting in a Bell pair. (c),d) X protocol. Instead of isolating the repeater lines, we directly X measure the vertices 4,5,8. The next step would be the Z-measurement of all neighborhood vertices of 1,9, but it is not necessary in this specific case. Thus, the X protocol requires fewer measurements compared to the repeater protocol and yields an additional four-node state, along with the required Bell pair.

Z measurements and remove intermediate vertices using X measurements. Since generating a repeater line is an essential step of these protocols, we will call them as *repeater protocol* from now onward.

An improvement over the repeater protocol described above was provided in Ref. [53]. The authors provided a more efficient method for establishing entangled states, where the efficiency of a protocol refers to the total number of measurements required to enact the protocol. The lesser the number of measurements needed, the greater the connections left in the graph, which could be used in subsequent rounds for further generation of specific entangled states. This protocol leverages the properties of X measurements on graph states and is aptly called the X *protocol* [see Figs. 1(a) and 1(d)]. For the Bell pair generation between two nodes, the protocol proceeds as follows: find the shortest path between two nodes with the minimum combined neighborhood path with the minimum number of neighbours), perform X measurements on all the intermediate vertices, and subsequent Z measurement of all the neighboring vertices of the two vertices. The X measurements connect the two nodes, as in the repeater protocol. The difference here is that the two nodes acquire additional neighbours during the X-measurement step, which increases the number of Z measurements required in the next step. The authors proved [53] that the total number of measurements required for the X protocol was nevertheless lesser than the repeater protocol. They also applied the X protocol to generate $|\text{GHZ}_3\rangle$ states among three specific vertices.

Now let us consider the problem of establishing GHZ states shared among more than three parties. As explained before, the above-mentioned methods cannot be generalized easily to the multiparty case. We now prove that one can extract $|\text{GHZ}_n\rangle$ from a connected graph, given the graph satisfies a vertex minor condition. The protocol will then be analyzed using specific examples to showcase their benefits and to compare with previously known results.

Theorem III.1. (Extraction of $|\text{GHZ}_n\rangle$ states): It is possible to extract an n-partite GHZ state from a graph state $|G\rangle$ when the underlying graph has a repeater line as vertex-minor, connecting all n nodes of the final GHZ state with an extra node in between every pair of $n-2$ intermediate nodes.

Given such a repeater line, the GHZ state can be obtained by performing sequential local complementations on all vertices except the two at both ends and subsequent Z measurement of all the neighboring vertices not part of the final state.

Proof. The proof is obtained by keeping track of the neighborhood of the nodes throughout the measurement process. For simplicity, let us assume the case where the required repeater line is isolated from the rest of the graph through some Z measurements. Let us denote vertices along the path as v_i, vertices at even positions as e_i and at odd positions by o_i(except those at both ends). We have $e_i = v_{2i}$ and $o_i = v_{2i+1}$.

Lemma III.2. After performing LC on every vertex up to v_i in an isolated repeater line, the neighborhood of v_{i+1} is given by $N_{v_{i+1}} = \{v_1, \dots, v_i, v_{i+2}\}$.

Proof. This can be easily proved through induction. After LC on v_2, $N_{v_3} = \{v_1, v_2, v_4\}$. Assume lemma to be true for n; after LC on v_n, $N_{v_{n+1}} = \{v_1, \dots, v_n, v_{n+2}\}$. At this point $N_{v_{n+2}} = \{v_{n+1}, v_{n+3}\}$. LC on v_{n+1} gives us

$$\begin{aligned} N_{v_{n+2}} &= N_{v_{n+1}} \cup \{v_{n+1}, v_{n+3}\} \backslash v_{n+2} \\ &= \{v_1, \dots, v_{n+1}, v_{n+3}\}, \end{aligned} \tag{1}$$

proving the lemma. This implies that LC on v_i connects v_{i+1} to every vertex before it in the repeater line. ■

Take any two vertices $e_i, e_j; i < j$. Since the choice of i, j is arbitrary, it suffices to prove that they remain connected at the end of the protocol. We can now look at how the edge connection between these vertices develops throughout the protocol. Note that, initially, e_i and e_j are not connected. There exists at least one odd vertex in between them. The two vertices are connected for the first time when one performs LC on the odd vertex o_{j-1} (Lemma III.2). Next LC is to be performed on e_j; which does not affect the connection. However, this operation connects o_j to e_i. Thus, the next LC, performed on o_j removes the edge between e_i and e_j. Since now e_{j+1} is connected to e_i and e_j and e_i, e_j are not connected to each other, LC on e_{j+1} rebuilds the edge between e_i and e_j. This pattern is followed by the rest of the protocol, where LC on odd vertices removes the edge and LC on even vertices adds the edge. Since the sequence of LC's ends with an even vertex, owing to the specific construction of the repeater line, e_i, e_j remains connected at the end of LC operation. Z measurements on odd vertices will not affect the connectivity of even vertices. Since this applies for any i, j with $i < j$, all n vertices are connected at the end of this protocol and we have the desired GHZ state. ■

Lemma III.3. (Generalized X protocol): Assuming the repeater line required by Theorem III.1 exists, performing X measurement on the odd vertices and subsequent Z measurement of all the neighboring vertices not part of the final state yields the desired GHZ state.

Proof. We will show how this generalized X protocol is equivalent to the protocol used to prove Theorem III.1. As before, we assume that the repeater line is isolated from the rest of the graph. Such a repeater line requires, by Theorem III.1, at least $2n-3$ vertices for constructing the $|\text{GHZ}_n\rangle$ state. Let's number the vertices sequentially and represent LC, Z, X measurements on vertex v_i as LC_i, Z_i, X_i, respectively. The protocol presented above can be then represented by

$$Z_3 Z_5 \cdots Z_{2n-7} Z_{2n-5} LC_{2n-4} LC_{2n-5} \cdots LC_3 LC_2.$$

Note that Z_i commutes with LC_j, since a measurement removes the node and all the edges connected to it. Rearranging, we get

$$LC_{2n-4}(Z_{2n-5} LC_{2n-5} LC_{2n-6}) \cdots (Z_5 LC_5 LC_4)(Z_3 LC_3 LC_2).$$

The terms in the bracket look similar to X measurement performed on node v_i, in addition a term corresponding to the final LC of the neighbor node v_{i-1},

$$X_i \equiv LC_{i-1} Z_i LC_i LC_{i-1}.$$

A key observation here is that, after the Z_i measurement, out of all the n vertices to be included in the final GHZ state, v_{i-1} is only connected to v_{i+1}. Even if we consider the case where the repeater line is not isolated, local complementation on v_{i-1} will only change the edge connectivity of its neighbors, which will be deleted anyway. So it does not matter if we perform the local complementation or not. The final LC, LC_{2n-4} can also be ignored since it is just a local operation on the final GHZ state itself. Hence we can rewrite the protocol to be

$$X_{2n-5} X_{2n-7} \cdots X_5 X_3.$$

In Fig. 2, we show an example of isolating the desired repeater line from an underlying 3×4 grid-graph to subsequently distill a GHZ5 state composed of the nodes 1,4,6,12,10. Note that depending on the underlying graph and the distribution of vertices, such a repeater line may or may not exist. In this case, the repeater line composed of the vertices 1,4,5,6,9,12,11,10 satisfies the conditions laid out in Theorem III.1, specifically, the existence of an extra node between the intermediate nodes 4,6, and 12. Note that the node 11 is unnecessary for the protocol and can be removed after isolating the repeater line. After we isolate the repeater line, there are two equivalent ways to generate the final GHZ state. In Fig. 3, sequential LC's are applied to the repeater line vertices. This connects every vertex that's supposed to be part of the final state to each other. Removing all the unnecessary vertices in the final step yields the required state. In Fig. 4, the X measurements are carried out on the vertices that are not part of the final state. Both methods are equivalent and result in the same final state.

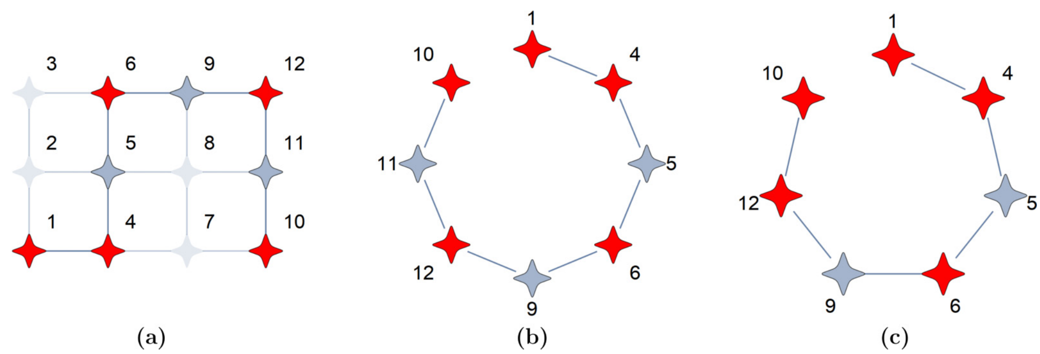

FIG. 2. Isolating the desired repeater line. (a) A 3 × 4 grid network. The highlighted path connects the vertices 1,4,6,12,10, which are to be part of the final GHZ state. Z measurement on the vertices 3,2,8,7 isolates this path from the rest of the graph. (b) The isolated path. The vertex 11 is not required for the protocol and we can remove it using an X measurement. (c) The repeater line as required by Theorem III.1. It contains the five nodes of the final GHZ state and extra nodes between the intermediate nodes 12,6,4.

In the above theorems and examples, we have presented a case where the repeater line is first isolated from the graph state to apply the protocol. This is unnecessary, and one can perform the protocol directly on the repeater line while embedded within the graph state and subsequently isolate the final state from the rest of the graph. To see this, consider the case where the repeater line is not isolated and we perform the above-stated protocol. Let v_i be an arbitrary vertex along the repeater line. Suppose at some point in the protocol we apply the LC operation on v_i. For any two neighbors u, w of v, the change in their edge relation due to LC_i is independent of other vertices in the graph (II.2). Combined with the fact that all LC operations in our protocol are applied along the vertices of the repeater line, this implies that the changes in edge relations among the vertices of the repeater line by applying the protocol is not influenced by how the repeater line is connected to the rest of the graph. This is quite similar to the contrast between the repeater protocol and X protocol. The authors [53] showed that operating on the repeater line before isolating the final state requires fewer measurements than if we go the other way around. We can prove a similar result for our generalized version. The proof of the following lemma is given in the Appendix.

Lemma III.4. The generalized X protocol performed before isolating the repeater line requires, at most, many measurements as the one where the repeater line is isolated first.

Proof. Proof of this theorem is given in the Appendix. ■

As an example, Fig. 5 shows an example where the X protocol is applied prior to the isolation of the repeater line. Extracting Bell pairs and $|\mathrm{GHZ}_3\rangle$ states with local operations is always possible in a connected graph [53]. Our theorem reflects this possibility since the requirement of "an extra node in between every pair of $n-2$ intermediate nodes" is trivially satisfied for $n = 2, 3$. In Ref. [53], a sufficient criterion for extracting $|\mathrm{GHZ}_4\rangle$ states was also provided. This special case ($n = 4$) of our generalized protocol is presented in Fig. 6. A crucial part of the protocol is the generation of the repeater line connecting the final four vertices 10,1,6,12, with an extra node between the two intermediate vertices 1,6 [Fig. 6(c)]. Thus, it satisfies the conditions of Theorem III.1, and the protocol proceeds by performing sequential LC and Z measurements, the same as in our protocol.

We note here that there is an even more efficient way of extracting the $|\mathrm{GHZ}_4\rangle$ state for this specific example. A downside of using the protocol in Fig. 6 is that it removes the possibility of extracting more entangled states from the same graph. Here, we show how this protocol can be modified to extract an extra Bell pair and the GHZ state from the same graph state (Fig. 7). Instead of isolating the repeater line, we perform a suitably chosen X measurement to modify the graph state to enable simultaneous extraction of multiple states. Essentially, it converts the original state, Fig. 7(a), to one of its vertex-minors, Fig. 7(b), such that it enables us to distill an extra Bell pair without disturbing the $|\mathrm{GHZ}_4\rangle$ extraction protocol.

So far we have considered the case where each node has just a single-qubit memory. We can extend the protocol to the case where there is no such limitation. Consider nonadjacent nodes $\{v_i\}$ for any i, with a suitable repeater line connecting them, each containing m_i qubit quantum memories. We now show how our protocol can be used to share a $|\mathrm{GHZ}_M\rangle$ state where $M = \sum m_i$.

Assume that arbitrary operations are allowed within a node. Using two-qubit gates and local rotations we can construct a $|\mathrm{GHZ}_{m_i}\rangle$, or equivalently, a star graph with m_i vertices at v_i. Let the central nodes of the star graphs be denoted as c_i. If there exists a repeater line connecting c_i, one can perform the X protocol to obtain the $|\mathrm{GHZ}_M\rangle$ state.

Intuitively, we can see why this is the case the following way. Remember that the X protocol applied on a line graph (with a single-qubit memory per vertex) results in a star graph (Fig. 4). Now for the case with multiple memories per node, we can think of the star graph at every node as being generated from a separate X protocol. This is equivalent to a case where some X measurements are already applied on a line graph (with a single qubit per vertex) prior to applying the X protocol on that graph. Note that the actual order of X measurements does not matter if we are measuring nonadjacent qubits, each of which can be assigned a distnict neighbor [44]. Each X measurement only updates the edge relations among its local neighborhood and the local neighborhood of one of its adjacent vertices. If we make sure that for every nonadjacent vertex to be X measured we can choose a distinct neighbor, then the X measurements commute with each

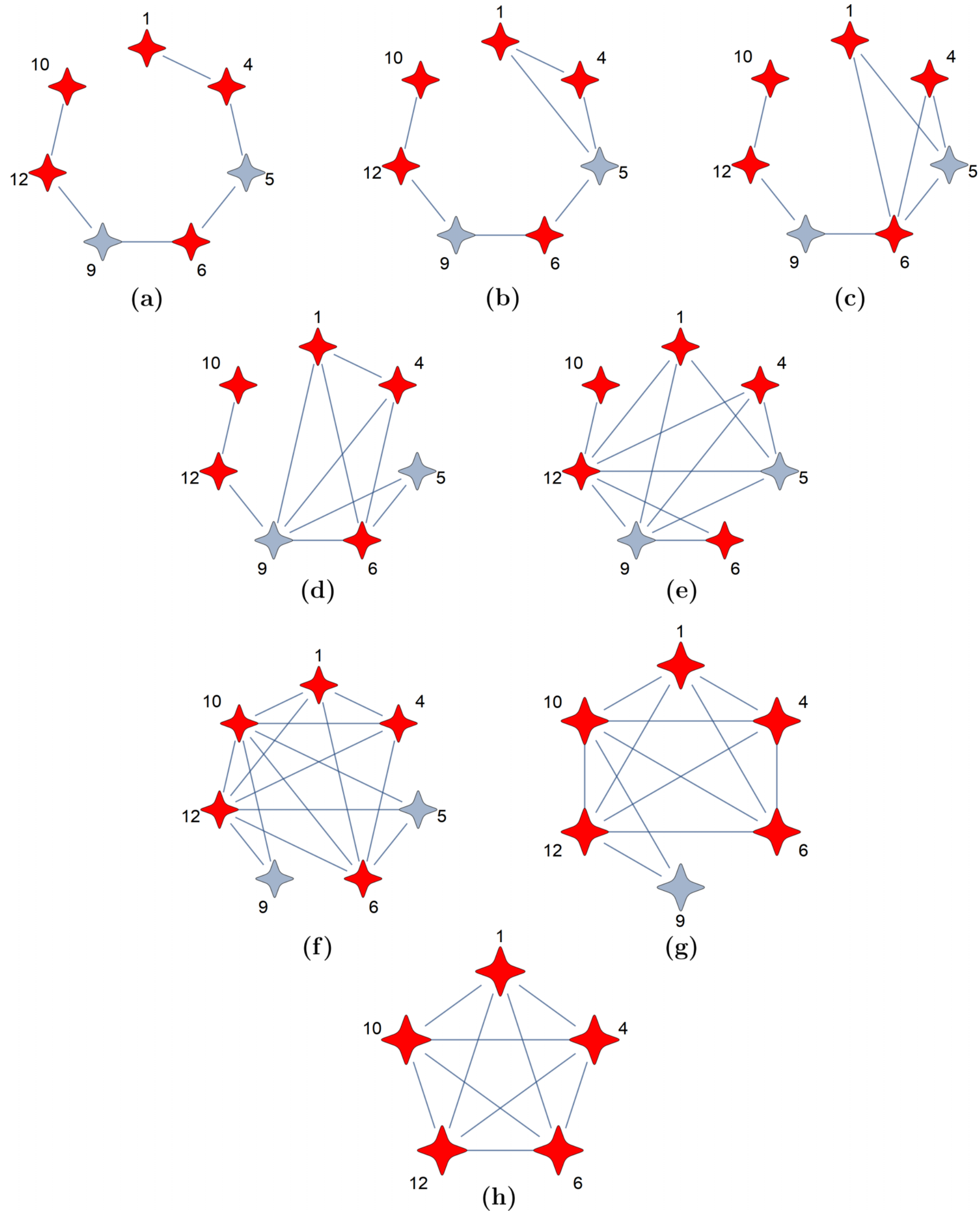

FIG. 3. Extracting GHZ5 state. (a) The isolated repeater line from Fig. 2. (b)–(f) Sequential *LC* on vertices 4,5,6,9,12. (g), (h) Z measurement of vertices 5,9.

other. Figure 8 illustrates this concept. Finally, we compare our results with the existing results on the size of the largest GHZ state extractable from a graph state. If we denote the number of vertices in the graph state as n, then for line graphs a bound of $n/2$ was conjectured in Ref. [58]. In other words, in Ref. [58], it was conjectured that to extract the $|\mathrm{GHZ}_n\rangle$ state, one would require a graph state with at least n vertices for a line graph. The X protocol beats this bound narrowly with a construction of the $|\mathrm{GHZ}_n\rangle$ state with a graph state of size (i.e., no of vertices) $\lfloor (n+3)/2 \rfloor$. This is the optimal value for line graphs [59].

For symmetric $n \times n$ grid graphs with n^2 vertices a bound of $\lceil n/2 \rceil^2$ was conjectured in [58]. We show in Fig. 9 that X protocol can at least achieve a size of $\lfloor (n+1)/4 \rfloor (3\lfloor (n-1)/2 \rfloor + 4) - 2$. The ratio of the sizes achieved by the X protocol and the one in Ref. [58] is $3/2$ as n tends to infinity. We can see an advantage for n as low as 3. In Fig. 9, we can see a best-case scenario where the ratio of the sizes is already maximum for $n = 7$. It is an open question whether this is the best possible result for grid graphs.

IV. GRID GRAPHS

Grid graphs belong to an important class of network architecture known as nearest-neighbor networks. Such networks are relevant to practical quantum communication since they connect nearest neighbors via physical links. Consequently, the quantum information only has to travel a short

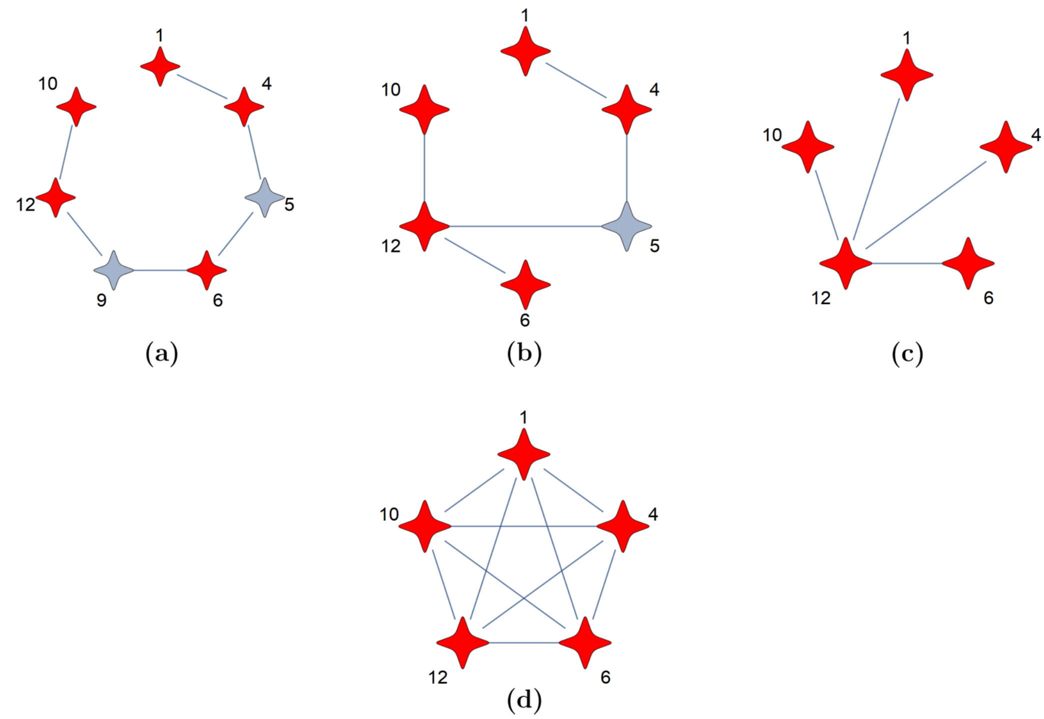

FIG. 4. Extracting GHZ5 state. (a) The isolated repeater line from vertex 5. (b) X measurement on vertex 9. (c) X measurement on vertex 5. (d) The final state obtained by performing LC on vertex 12.

distance, thus minimizing transmission losses and errors. Nearest neighbor networks like rings, lines, and grid graphs have been studied under different scenarios, especially in communication bottlenecks. In the simplest scenario, a bottleneck arises in a network when two pairs of nodes intend to share a Bell pair over a common edge. It was shown in Ref. [60] that ring and line networks cannot overcome such bottlenecks, whereas it has been shown to be possible in grid graphs in the case of a "*butterfly network*" [53,61,62].

This section will show how symmetry in grid graphs can be utilized in the entanglement routing problem. We will explore the simplest routing task of establishing a Bell pair between two distant nodes (with no direct physical link) in a connected graph. A naive solution to this would be the repeater protocol. We have already mentioned that a more efficient approach was discussed in Ref. [53], which we referred to as the X protocol. The authors proved that for the shortest with the minimum combined neighbourhood path, the X protocol requires fewer measurements than the repeater protocol.

However, there is still an ambiguity left on the *choice* of the path to make, as the minimum-combined neighborhood

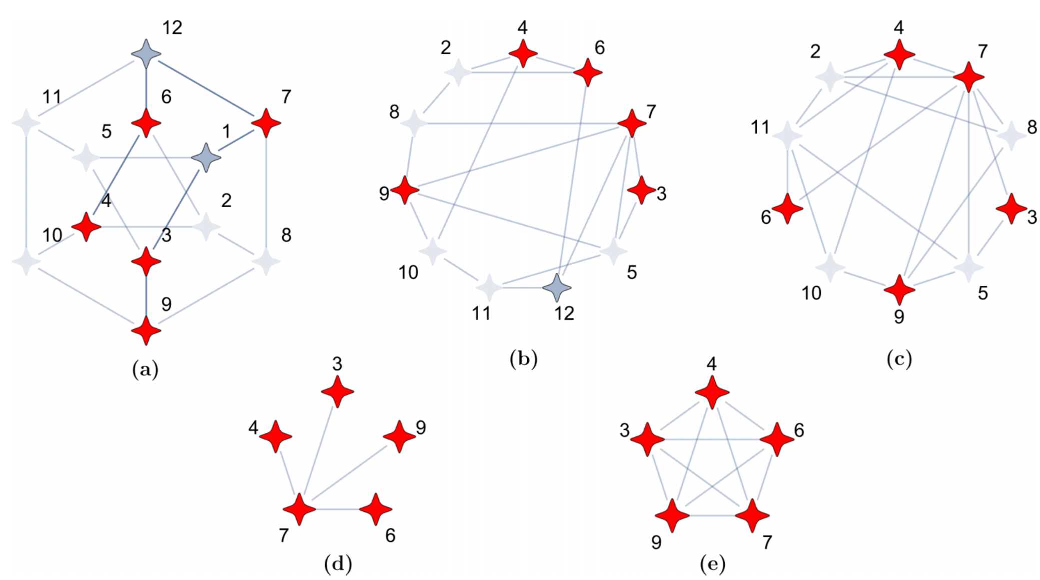

FIG. 5. (a) Network with graph corresponding to generalized Petersen graph $P_{6,4}$. (b) X measurement on 1. (c) X measurement on 12. (d) Z measurement on all the neighborhood vertices of the red nodes. (e) LC operation on 7.

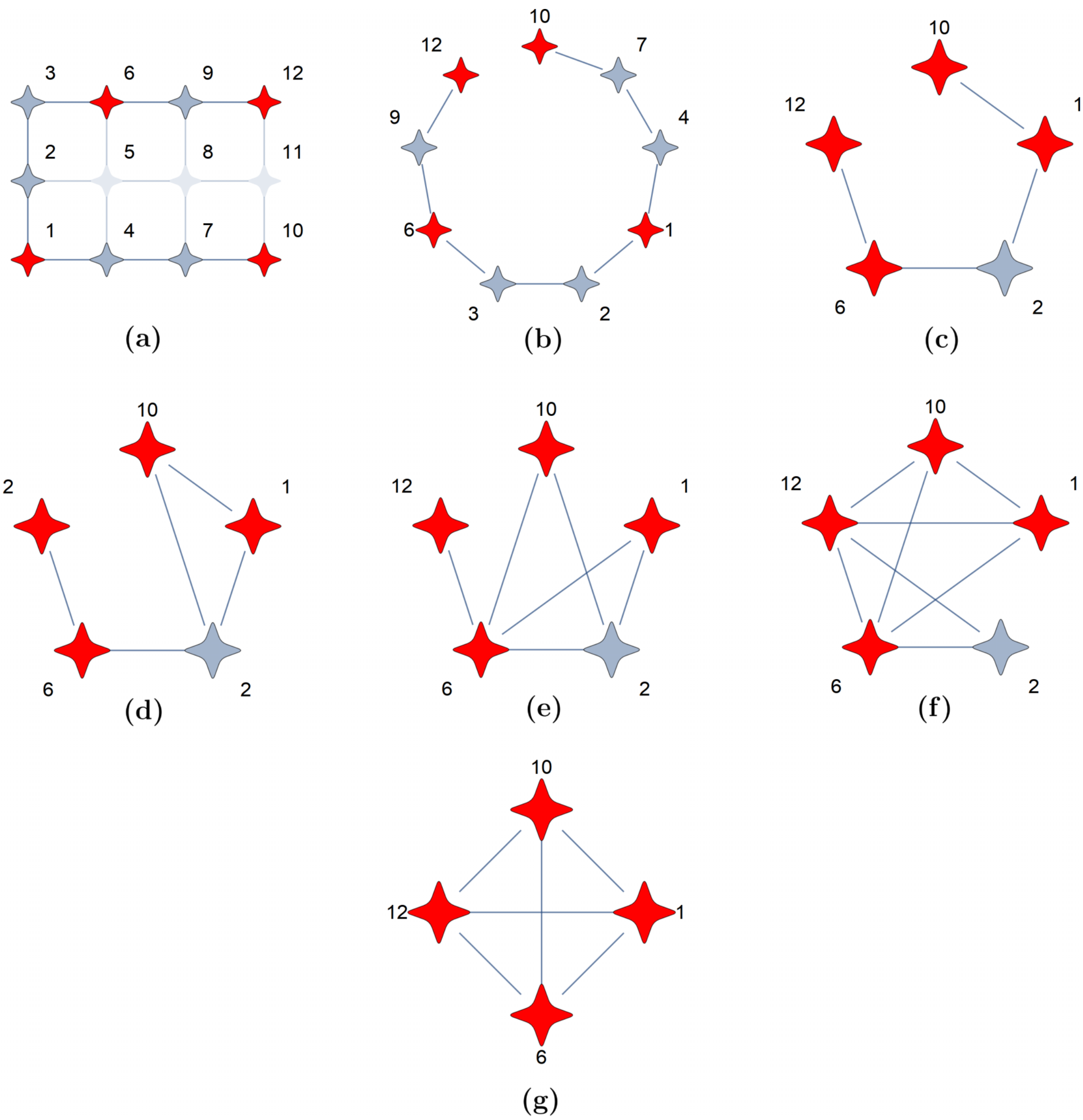

FIG. 6. Extracting $|GHZ_4\rangle$ state; example given in Ref. [53]. (a) Identify a suitable path connecting the vertices 12,6,1,10 that are to be part of the final state. (b) Isolate the path using Z measurements on vertices 5,8,11. (c) Appropriate measurements on vertices 9,3,4,7 to reach this five vertex graph. (d)–(f) Sequential LC on 1,2,6. (g) Z measurement of 2 yields the desired $|GHZ_4\rangle$ state.

path is not always unique. To illustrate this point, in Fig. 10, we show all the different paths (with minimum length and combined neighborhood) one can have given a graph and a pair of nodes. The theorems in Ref. [53] just tell us that, given any of these paths, the X protocol would perform better than the repeater protocol; it does not provide any information on the ideal path to choose. It is unclear whether all the paths are equivalent or if one performs better. Thus, a set of open questions remain, and in what follows, we will address these questions.

In the following, we define a property to these paths, enabling us to define a "better" path qualitatively. We use the concept of majorization, an ordering relation on real vectors. Majorization has already seen extensive applications in quantum information, including entanglement theory [63] and the formulation of resource theories [64]. Here, we will use this tool to judge the entanglement routing paths in a quantum network qualitatively. We associate a vector to all the feasible paths, referred to as the *path vector*. Given a set of such path vectors, we can impose an ordering relation based on the majorization relation. This would enable us to infer the best path to choose for entanglement routing.

The first step towards defining the path vector is associating a sense of direction within the grid graph. This is done easily by viewing the grid graph on a Cartesian plane and locating every vertex on the coordinates $(x, y); x, y \in \mathbb{N}$, with adjacent vertices separated by unit distance on either of the coordinates. Every edge in this setting will be parallel to the x or the y axis. This implies that every path on a grid graph can be represented using a sequence of edges along the x and y directions. Since we are only concerned with the shortest path between two nodes, without loss of generality, we can restrict

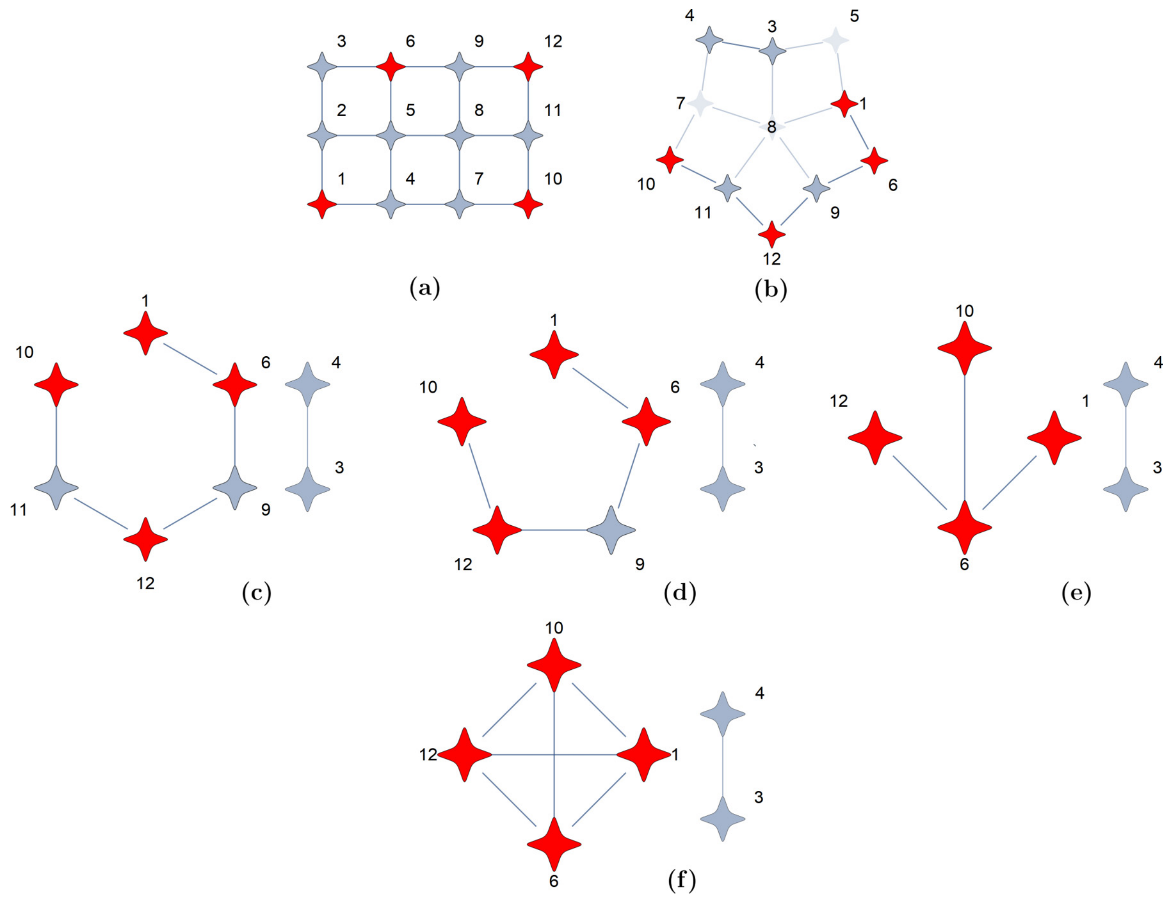

FIG. 7. Extracting $|\mathrm{GHZ}_4\rangle$ state and a Bell pair. (a) The same underlying graph and vertices are to be connected, as in Fig. 6. (b) X measurement on 2 converts the grid state to one of its vertex minors. (c) Z measurements on 7,8,5. (d) X measurement on 11. (e) X-measurement on 9. (f) *LC* on 6.

ourselves to positive x and y. We now have the necessary ingredients to define a path vector.

Suppose we have two vertices a and b, with the coordinates (x, y) and (x', y'). Define $D_x = |x' - x|$ and $D_y = |y' - y|$. $D = D_x + D_y$ is the number of edges in the shortest path connecting a, b. A path vector $\mathbf{s}$ given by $(s_{x_1}, s_{y_1}, s_{x_2}, s_{y_2}, \ldots, s_{x_{D_x}}, s_{y_{D_y}})$ defines a shortest path between a and b iff $s_{x_1} + s_{x_2} + \cdots + s_{x_{D_x}} = D_x$ and $s_{y_1} + s_{y_2} + \cdots + s_{y_{D_y}} = D_y$. Here, s_{x_i} is the number of consecutive edges the path covers in the x direction, after which it changes direction and covers s_{y_i} number of edges in the y direction. Hence every shortest path will have a unique vector. We will represent the path with path vector $\mathbf{s}$ as S.

Definition IV.1. (Majorization): Given $\mathbf{s}, \mathbf{t} \in \mathbb{R}^d$ we say that $\mathbf{t}$ is majorized by $\mathbf{s}$ (written as $\mathbf{s} \succ \mathbf{t}$) iff

$$\sum_{i=1}^{k} s_i^{\downarrow} \geqslant \sum_{i=1}^{k} t_i^{\downarrow} \quad \text{for } k = 1, \ldots, d-1 \tag{2}$$

$$\sum_{i=1}^{d} s_i = \sum_{i=1}^{d} t_i, \tag{3}$$

where $\mathbf{s}^{\downarrow} \in \mathbb{R}^d$ is the vector $\mathbf{s}$ with the same scalar components, but sorted in descending order. For example, if $\mathbf{s} = (2, 1, 3)$ then $\mathbf{s}^{\downarrow} = (3, 2, 1)$. A similar definition holds for $\mathbf{t}^{\downarrow}$.

Theorem IV.1. Given path vectors $\mathbf{s}$, $\mathbf{t}$ and $\mathbf{s} \succ \mathbf{t}$, the X protocol along T requires, at most, as many measurements as the one along S.

Proof. Proof of this theorem is given in the Appendix. ■

For example, in Fig. 10, we show three different paths on a 4×4 grid graph to establish a Bell pair between the vertices 1,16. The length and combined neighborhood of all paths are the same. We show the end result of the X protocol and the corresponding path vector for each path. From the figure, it is clear that, given any pair of paths, one with the majorized path vector produces better results in the X protocol.

V. DISCUSSIONS

This paper provides a protocol for extracting multipartite entangled states from quantum networks using just local measurements. This work extends the results found in Ref. [53] in which the authors provided methods for extracting $|\mathrm{GHZ}_n\rangle$ for $n \leqslant 4$. Here, we provided a general method that works for *any* n. Our protocol is applicable on a shared network state with a single qubit per location and is hence favorable in terms of the repeater memory required compared to previous protocols [14]. It relies on constructing a repeater line connecting the final vertices and local measurements on the nodes in between. Another important contribution of this

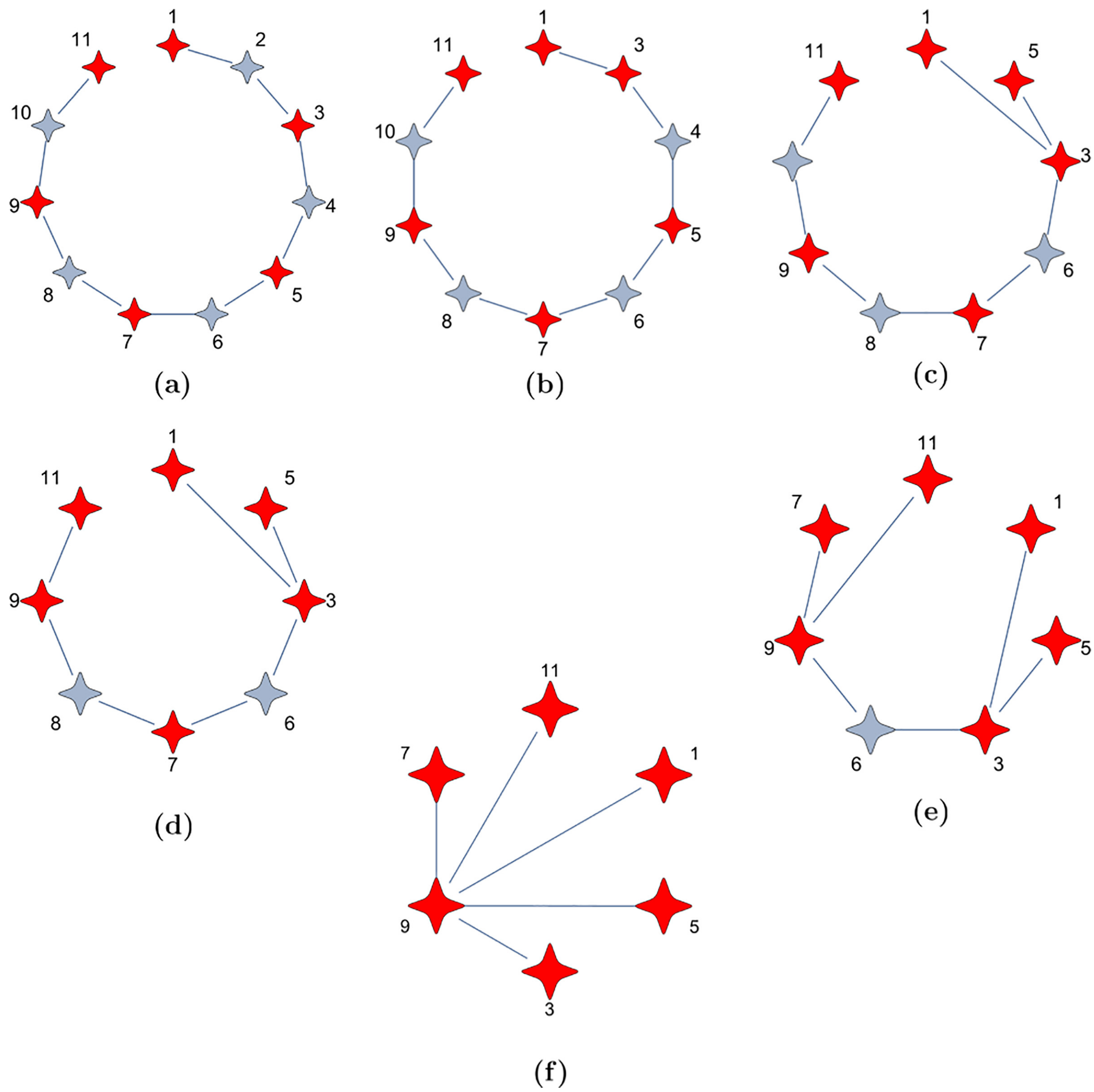

FIG. 8. X measurements on a repeater line need not be sequential. Every vertex to be measured can be assigned a unique neighbor. (a) A repeater line with red nodes to be part of the final state. (b) X measurement on node 2 (with chosen neighbor 1). (c) X measurement on node 4 (with chosen neighbor 5). (d) X measurement on node 10 (with chosen neighbor 11). (e) X measurement on node 8 (with chosen neighbor 7). (f) Final X measurement on node 6 (with chosen neighbor 3).

work is the key observation that the protocol does not mandate the repeater line be removed from the underlying graph state, which reduces the number of measurements required for the overall protocol. Note that this protocol could still be applied if we allow for multiple qubit memories per user. We also analyzed nearest-neighbor networks and show how their structure and symmetry can help us devise better protocols for entanglement routing.

This work is expected to open a window for an investigation into a plethora of new problems. For example, it would be worthwhile to explore whether the protocol could be adapted to incorporate all-photonic quantum repeaters [5]. Such memory-less repeaters were introduced to establish entanglement between two distant nodes, where the repeaters would use cluster states to connect neighboring stations. Measurements on such cluster states would eventually connect the distant nodes and establish entanglement between them. Since our protocol also requires just local X measurements along a repeater line, it would be interesting to see how the all-photonic repeaters could be modified to fit our protocol. Proof-of-principle experiments based on this concept have been demonstrated successfully in recent years [7,65], and its resource efficiency with matter memories has been characterized [66]. This makes us optimistic about the practical realization of our work in a broad domain.

Recently, Ref. [67] proposed a protocol for anonymous conference key agreement among any three participants of a linear network. The users need only to share Bell pairs with their neighbors and avoid the necessity of a central server sharing multipartite states. The network users perform local measurements to extract the $|GHZ_3\rangle$ state among the participants, which can subsequently be used for key agreement.

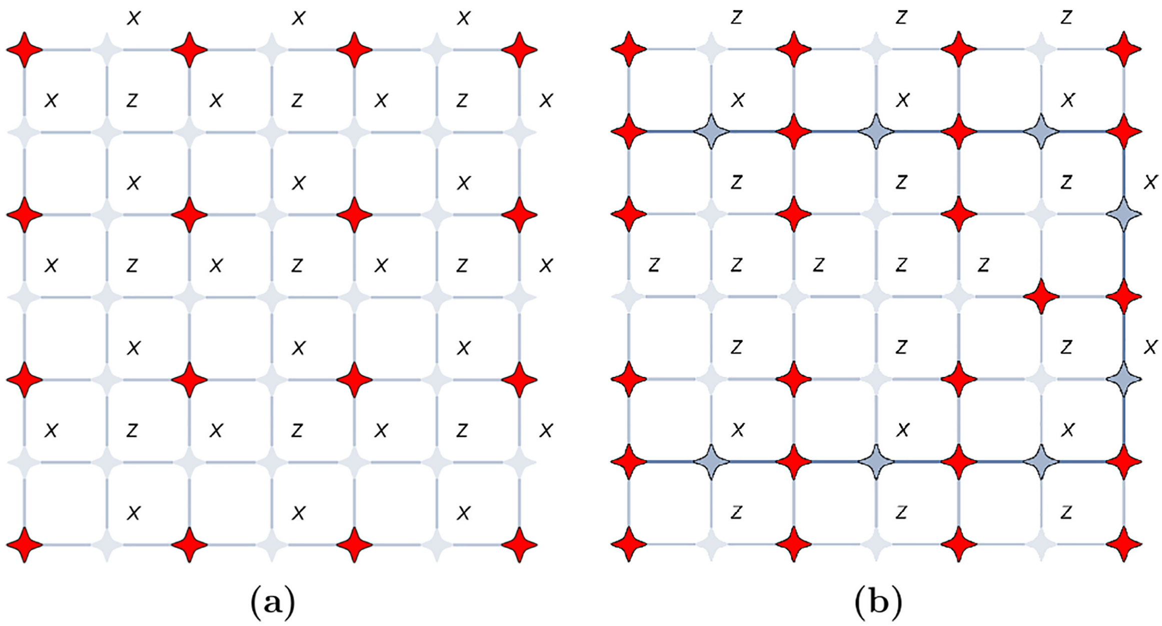

FIG. 9. (a) Protocol in Ref. [58] for extracting $|\mathrm{GHZ}_{16}\rangle$. (b) X protocol for extracting $|\mathrm{GHZ}_{24}\rangle$. The construction can be generalized to any $n \times n$ grid graph with odd n. It involves constructing a repeater line with interleaved star graphs with three vertices horizontally and joining them in the last column with star graphs of size two. If we denote by $x = \lfloor (n-1)/2 \rfloor$ the number of three vertex star graphs possible in a row and $y = \lfloor (n+1)/4 \rfloor$ as the number of such graphs in a column, then the size of the final GHZ state is given by $3xy + 2y + 2(y-1) = y(3x+4) - 2$.

Interestingly, the protocol introduced in this work can be used to generate $|\mathrm{GHZ}_n\rangle$ states from a linear network. Further, It would be interesting to see if we can extend the concepts laid out in Ref. [67] to propose a similar protocol for n parties.

A major limitation of this work is that it assumes a static network topology, i.e., the protocol assumes a global knowledge of the state of the network. Keeping in mind the finite coherence time of quantum memories and communication delay between adjacent nodes, an ideal routing protocol should only make use of the local link knowledge of nodes i.e., nodes are only aware if they were able to share an entangled pair between its immediate neighbors. In the bipartite routing scenario, the authors of Ref. [38] calculated the entanglement generation rate under the constraint of local link knowledge in a network. They showed that, by taking advantage of multiple routing paths in a network, the rate of entanglement generation can supersede the same achievable using a linear repeater chain. Note that their results also rely on generating a linear chain of nodes connecting the final nodes. Since our protocol also relies on such a linear chain, a natural line of research would be to consider the multipartite entanglement generation rates using our protocol with just the local link knowledge. We leave that as a direction of future research.

Note added. Results similar to those presented in this work were also independently discovered recently [59].

ACKNOWLEDGMENTS

V.M. and A.P. acknowledge support from the QUEST scheme of the Interdisciplinary Cyber-Physical Systems (ICPS) program of the Department of Science and Technology (DST), India, Grant No. DST/ICPS/QuST/Theme-1/2019/14 (Q80). A.P. acknowledges support from the QUEST scheme of Interdisciplinary Cyber-Physical Systems (ICPS) program of the Department of Science and Technology (DST), India, Grant No. DST/ICPS/QuST/Theme-1/2019/6 (Q46). V.M. acknowledges support from The Galician Regional Government (consolidation of Research Units: AtlantTIC), The Spanish Ministry of Economy and Competitiveness (MINECO), and the Fondo Europeo de Desarrollo Regional (FEDER) through Grant No. PID2020-118178RB-C21, MICIN with funding from the European Union NextGenerationEU (PRTR-C17.I1) and the Galician Regional Government with its own funding through the Planes Complementarios de I + D + I con las Comunidades Autónomas in Quantum Communication and The European Union's Horizon Europe Framework Program under the Marie SklodowskaCurie Grant No. 101072637 (Project QSI) and the project Quantum Security Networks Partnership (QSNP, Grant Agreement No. 101114043). The authors also thank Kishore Thapliyal for his interest and feedback on the work.

The code used to generate the figures will be made available to the interested reader upon reasonable request.

APPENDIX A: PROOF OF LEMMA III.4

1. Lemma III.4

The generalized X protocol performed before isolating the repeater line requires, at most, as many measurements as the one where the repeater line is isolated first.

Proof. Let us count the number of measurements required for the protocol in both cases, the case where the repeater line is isolated from the graph before the X measurements and one where it is not isolated. Assume that we are trying to generate a $|\mathrm{GHZ}_n\rangle$ state. By Theorem III.1, an appropriate repeater line

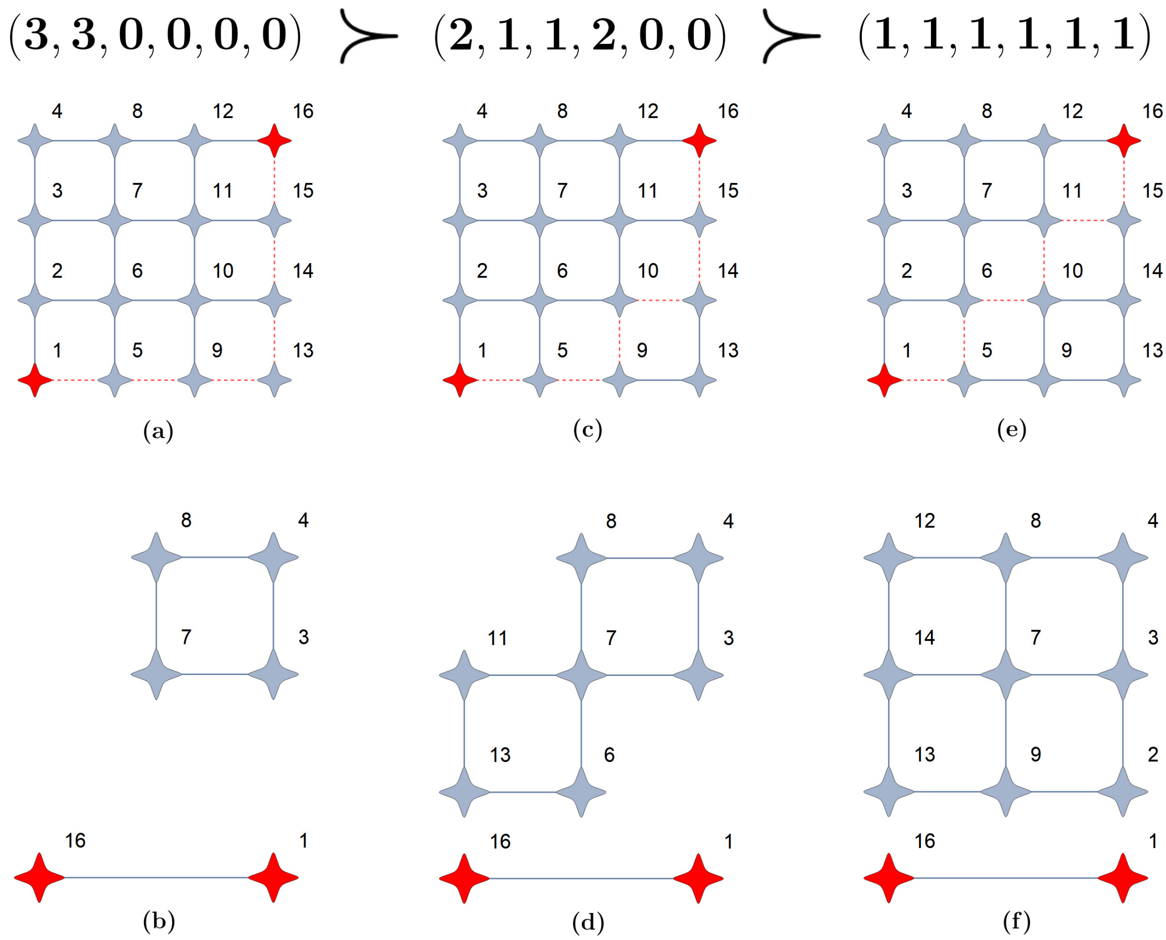

FIG. 10. Entanglement routing paths and their end-products. (a), (b) X protocol is performed along the path 1,5,9,13,14,15,16. The path is equivalently represented by the vector (3,3,0,0,0,0). In addition to the desired Bell pair between 1,16, we also obtain a 2×2 grid state. (c), (d) A different path that requires a lesser amount of measurements than the previous path. This is evident from the higher number of connected vertices left in the graph. (e), (f) The optimal path to perform the X protocol. The path vector (1,1,1,1,1,1) corresponding to this path is majorized by every other path. By Theorem IV.1, this path maximizes the amount of entanglement left in the graph.

should contain at least $2n-3$ vertices. In the following, we denote by $N_{v_i}^{(t)}$ the neighborhood of node v_i after the tth Pauli measurement is performed on the initially given graph state.

a. With isolation

In this case one requires $|N_{v_1}^0 \cup \cdots \cup N_{v_{2n-3}}^0| - (2n-3)$ measurements for isolating the repeater line. The first term includes the neighborhood vertices of all the vertices on the repeater line. However, this also includes the $2n-3$ vertices themselves. Since we are not measuring them at this stage, the second term accounts for this. After isolating, we need to perform the protocol on the repeater line. This involves $(n-3)$ X measurements of all the extra nodes. Thus, in total, we require $|N_{v_1}^0 \cup \cdots \cup N_{v_{2n-3}}^0| - n$ measurements.

b. Without isolation

Here, we first perform the X measurements of all the intermediate nodes. This step takes $n-3$ measurements, the same as before. After this step, we need to isolate the n-party state from the rest of the graph. This requires $|N_{v_1}^{n-3} \cup N_{v_2}^{n-3} \cup \cdots \cup N_{v_{2n-4}}^{n-3} \cup N_{v_{2n-3}}^{n-3}| - n$ measurements. The term in this expression accounts for the updated neighborhood vertices of the n vertices that are part of the final state after the X measurements on the repeater line. Since this also includes the n vertices themselves, we subtract it. Thus, the protocol requires a total of $|N_{v_1}^{n-3} \cup N_{v_2}^{n-3} \cup \cdots \cup N_{v_{2n-4}}^{n-3} \cup N_{v_{2n-3}}^{n-3}| - 3$ measurements.

Now, all we need to prove is that

$$\begin{aligned} &\left|N_{v_1}^{n-3} \cup N_{v_2}^{n-3} \cdots N_{v_{2n-4}}^{n-3} \cup N_{v_{2n-3}}^{n-3}\right| \\ &\quad \leqslant \left|N_{v_1}^{0} \cup \cdots \cup N_{v_{2n-3}}^{0}\right| - (n-3). \end{aligned} \tag{A1}$$

A crucial observation here is that X measurements on the repeater line do not change the combined neighborhood of the repeater line, except for the number of deleted vertices. This implies that

$$N_{v_1}^{n-3} \cup N_{v_2}^{n-3} \cdots N_{v_{2n-4}}^{n-3} \cup N_{v_{2n-3}}^{n-3} \subset N_{v_1}^{0} \cup \cdots \cup N_{v_{2n-3}}^{0}.$$

The subset relation is proper since the left-hand side (LHS) does not contain the $n-3$ vertices in the right-hand side (RHS) that were X measured. This proves Eq. (3) and hence the lemma. ■

APPENDIX B: PROOF OF THEOREM IV.1

1. Theorem IV.1

Given path vectors $\mathbf{s}$, $\mathbf{t}$ and $\mathbf{s} \succ \mathbf{t}$, the X protocol along T requires, at most, as many measurements as the one along S.

Proof. Given two path vectors, one being majorized by the other implies that the path contains fewer consecutive edges along a particular direction. The majorized path thus involves more changes in direction. A direct consequence is that a higher number of alternating vertices along the path share a common neighbor. We show how the expressions for the total number of measurements derived in the supplementary information found in Ref. [53] relate to the neighborhood intersections of vertices along the path.

Briefly recalling, in the X protocol, we first measure all the intermediate nodes along the path in X basis and subsequently Z measure all the neighbors of the connected pair. If the path contains l nodes, we require $(l-2)$ number of X measurements and some number of Z measurements (depending on the number of neighbors of the connected pair). In the Supplementary Material of Ref. [53], the authors derived an expression for the total number of Z measurements Eqs. (16) and (17) of the Supplementary Material [53], given by

$$N_{v_1}^{(l-2)} = \left(N_{v_{l-1}}^{(0)} \cup N_{v_1}^{(l-4)}\right)\setminus\left(N_{v_{l-1}}^{(0)} \cap N_{v_1}^{(l-4)}\right),$$
$$N_{v_l}^{(l-2)} = \{v_1\} \cup \left(N_{v_l}^{(0)} \cup N_{v_1}^{(l-3)}\right)\setminus\left(N_{v_l}^{(0)} \cap N_{v_1}^{(l-3)}\right). \quad \text{(B1)}$$

Since they only considered the shortest path while proving this result, the path length is fixed, and the number of intermediate measurements required is the same for the different paths. Thus, we need to focus only on the number of measurements required to isolate the endpoints v_1 and v_l. Let us first consider the neighborhood of the first vertex v_1 after all the X measurements

$$N_{v_1}^{(l-2)} = \left(N_{v_{l-1}}^{(0)} \cup N_{v_1}^{(l-4)}\right)\setminus\left(N_{v_{l-1}}^{(0)} \cap N_{v_1}^{(l-4)}\right).$$

It is clear that greater the intersection between the terms $N_{v_{l-1}}^{(0)}$ and $N_{v_1}^{(l-4)}$, the lesser the cardinality of $N_{v_1}^{(l-2)}$.

Expanding $N_{v_1}^{(l-4)}$ using Eq. (2), we obtain

$$N_{v_1}^{(l-2)} = N_{v_{l-1}}^{(0)} \cup \left[\left(N_{v_{l-3}}^{(0)} \cup N_{v_1}^{(l-6)}\right)\setminus\left(N_{v_{l-3}}^{(0)} \cap N_{v_1}^{(l-6)}\right)\right]\setminus$$
$$N_{v_{l-1}}^{(0)} \cap \left[\left(N_{v_{l-3}}^{(0)} \cup N_{v_1}^{(l-6)}\right)\setminus\left(N_{v_{l-3}}^{(0)} \cap N_{v_1}^{(l-6)}\right)\right]. \quad \text{(B2)}$$

Consider the second half of the above expression

$$N_{v_{l-1}}^{(0)} \cap \left[\left(N_{v_{l-3}}^{(0)} \cup N_{v_1}^{(l-6)}\right)\setminus\left(N_{v_{l-3}}^{(0)} \cap N_{v_1}^{(l-6)}\right)\right].$$

Using the recursive formula Eq. (2), one sees that $N_{v_1}^{(l-6)}$, when expanded, contains terms of the form $N_{v_{l-5}}^{(0)}, N_{v_{l-7}}^{(0)}, \ldots$. Since we are restricting ourselves to the shortest paths in a grid graph, none of those terms will have nonempty intersections with $N_{v_{l-1}}^{(0)}$. Thus, the above expression reduces to

$$N_{v_{l-1}}^{(0)} \cap N_{v_{l-3}}^{(0)}. \quad \text{(B3)}$$

Now, for the first half of Eq. (3)

$$N_{v_{l-1}}^{(0)} \cup \left[\left(N_{v_{l-3}}^{(0)} \cup N_{v_1}^{(l-6)}\right)\setminus\left(N_{v_{l-3}}^{(0)} \cap N_{v_1}^{(l-6)}\right)\right].$$

Since $N_{v_{l-1}}^{(0)}$ has no intersection with the term $(N_{v_{l-3}}^{(0)} \cap N_{v_1}^{(l-6)})$, we can rewrite the above expression as

$$\left(N_{v_{l-1}}^{(0)} \cup N_{v_{l-3}}^{(0)} \cup N_{v_1}^{(l-6)}\right)\setminus\left(N_{v_{l-3}}^{(0)} \cap N_{v_1}^{(l-6)}\right).$$

Since $N_{v_{l-3}}^{(0)}$ only intersects with $N_{v_{l-5}}^{(0)}$ out of all the terms in the expansion of $N_{v_1}^{(l-6)}$, this becomes

$$\left(N_{v_{l-1}}^{(0)} \cup N_{v_{l-3}}^{(0)} \cup N_{v_1}^{(l-6)}\right)\setminus\left(N_{v_{l-3}}^{(0)} \cap N_{v_{l-5}}^{(0)}\right).$$

One can keep applying the same type of argument to terms of the form $N_{v_1}^{(l\neq 0)}$, and together with Eq. (3), we get

$$N_{v_1}^{(l-2)} = \left(N_{v_{l-1}}^{(0)} \cup N_{v_{l-3}}^{(0)} \cup N_{v_{l-5}}^{(0)} \cup \cdots\right)\setminus$$
$$\left(N_{v_{l-1}}^{(0)} \cap N_{v_{l-3}}^{(0)}\right)\setminus\left(N_{v_{l-3}}^{(0)} \cap N_{v_{l-5}}^{(0)}\right)\cdots. \quad \text{(B4)}$$

Similiarly for $N_{v_l}^{(l-2)}$,

$$N_{v_l}^{(l-2)} = \left(N_{v_l}^{(0)} \cup N_{v_{l-2}}^{(0)} \cup N_{v_{l-4}}^{(0)} \cup \cdots\right)\setminus$$
$$\left(N_{v_l}^{(0)} \cap N_{v_{l-2}}^{(0)}\right)\setminus\left(N_{v_{l-2}}^{(0)} \cap N_{v_{l-4}}^{(0)}\right)\cdots. \quad \text{(B5)}$$

Thus the total Z measurements required becomes

$$\left|N_{v_1}^{(l-2)} \cup N_{v_l}^{(l-2)}\right| = \left|N_{v_l}^{(0)} \cup N_{v_{l-1}}^{(0)} \cup N_{v_{l-2}}^{(0)} \cup \cdots \cup N_{v_1}^{(0)}\right|$$
$$- \left|\left(N_{v_l}^{(0)} \cap N_{v_{l-2}}^{(0)}\right) \cup \left(N_{v_{l-1}}^{(0)} \cap N_{v_{l-3}}^{(0)}\right)\right.$$
$$\left.\times \cup \cdots \cup \left(N_{v_1}^{(0)} \cap N_{v_3}^{(0)}\right)\right|. \quad \text{(B6)}$$

The first term in the above expression is the combined neighborhood of the path and the second term is the sum of intersections between alternate vertices. For the shortest path in a grid graph, the expression is minimized when the number of neighborhood intersections of vertices on the path is maximized. ■

[1] J.-P. Chen, C. Zhang, Y. Liu *et al.*, Twin-field quantum key distribution over a 511 km optical fibre linking two distant metropolitan areas, Nat. Photon. **15**, 570 (2021).

[2] M. Avesani, L. Calderaro, M. Schiavon *et al.*, Full daylight quantum-key-distribution at 1550 nm enabled by integrated silicon photonics, npj Quantum Inf. **7**, 93 (2021).

[3] S. Pirandola, R. Laurenza, C. Ottaviani, and L. Banchi, Fundamental limits of repeaterless quantum communications, Nat. Commun. **8**, 15043 (2017).

[4] N. Sangouard, C. Simon, H. de Riedmatten, and N. Gisin, Quantum repeaters based on atomic ensembles and linear optics, Rev. Mod. Phys. **83**, 33 (2011).

[5] K. Azuma, K. Tamaki, and H.-K. Lo, All-photonic quantum repeaters, Nat. Commun. **6**, 6787 (2015).

[6] Z.-S. Yuan, Y.-A. Chen, B. Zhao *et al.*, Experimental demonstration of a BDCZ quantum repeater node, Nature (London) **454**, 1098 (2008).

[7] Z.-D. Li, R. Zhang, X.-F. Yin *et al.*, Experimental quantum repeater without quantum memory, Nat. Photon. **13**, 644 (2019).

[8] S. Langenfeld, P. Thomas, O. Morin, and G. Rempe, Quantum repeater node demonstrating unconditionally secure key distribution, Phys. Rev. Lett. **126**, 230506 (2021).

[9] S.-K. Liao, W.-Q. Cai, J. Handsteiner *et al.*, Satellite-relayed intercontinental quantum network, Phys. Rev. Lett. **120**, 030501 (2018).

[10] J.-P. Chen, C. Zhang, Y. Liu *et al.*, Quantum key distribution over 658 km fiber with distributed vibration sensing, Phys. Rev. Lett. **128**, 180502 (2022).

[11] Y.-A. Chen, Q. Zhang, T.-Y. Chen *et al.*, An integrated space-to-ground quantum communication network over 4,600 kilometres, Nature (London) **589**, 214 (2021).

[12] C. Simon, Towards a global quantum network, Nat. Photon. **11**, 678 (2017).

[13] H. Lu *et al.*, Experimental quantum network coding, npj Quantum Inf. **5**, 89 (2019).

[14] C. Meignant, D. Markham, and F. Grosshans, Distributing graph states over arbitrary quantum networks, Phys. Rev. A **100**, 052333 (2019).

[15] S. Bäuml, K. Azuma, G. Kato *et al.*, Linear programs for entanglement and key distribution in the quantum internet, Commun. Phys. **3**, 55 (2020).

[16] V. Mannalath and A. Pathak, Entanglement routing and bottlenecks in grid networks, arXiv:2211.12535.

[17] A. Dahlberg, J. Helsen, and S. Wehner, Transforming graph states to Bell-pairs is NP-Complete, Quantum **4**, 348 (2020).

[18] M. Hillery, V. Bužek, and A. Berthiaume, Quantum secret sharing, Phys. Rev. A **59**, 1829 (1999).

[19] S. Gaertner, C. Kurtsiefer, M. Bourennane, and H. Weinfurter, Experimental demonstration of four-party quantum secret sharing, Phys. Rev. Lett. **98**, 020503 (2007).

[20] W. Tittel, H. Zbinden, and N. Gisin, Experimental demonstration of quantum secret sharing, Phys. Rev. A **63**, 042301 (2001).

[21] L. Xiao, L. Long, G., F.-G. Deng *et al.*, Efficient multiparty quantum-secret-sharing schemes, Phys. Rev. A **69**, 052307 (2004).

[22] M. Hillery, M. Ziman, V. Bužek *et al.*, Towards quantum-based privacy and voting, Phys. Lett. A **349**, 75 (2006).

[23] K. Thapliyal, R. D. Sharma, and A. Pathak, Protocols for quantum binary voting, Int. J. Quantum Inform. **15**, 1750007 (2017).

[24] S. Mishra, K. Thapliyal, A. Parakh, and A. Patha, Quantum anonymous veto: A set of new protocols, EPJ Quantum Technol. **9**, 14 (2022).

[25] G. Murta, F. Grasselli, H. Kampermann *et al.*, Quantum conference key agreement: A review, Adv. Quantum Technol. **3**, 2000025 (2020).

[26] M. Proietti, J. Ho, F. Grasselli *et al.*, Experimental quantum conference key agreement, Sci. Adv. **7**, eabe0395 (2021).

[27] F. Hahn, J. de Jong, and A. Pappa, Anonymous quantum conference key agreement, PRX Quantum **1**, 020325 (2020).

[28] A. Banerjee, K. Thapliyal, C. Shukla, and A. Pathak, Quantum conference, Quantum Info. Proc. **17**, 161 (2018).

[29] H. Buhrman and H. Röhrig, Distributed Quantum Computing, in *Mathematical Foundations of Computer Science 2003* (Springer, Berlin, 2003), pp. 1–20.

[30] Y. L. Lim, A. Beige, and L. C. Kwek, Repeat-until-success linear optics distributed quantum computing, Phys. Rev. Lett. **95**, 030505 (2005).

[31] I. L. Chuang, Quantum algorithm for distributed clock synchronization, Phys. Rev. Lett. **85**, 2006 (2000).

[32] R. Jozsa, D. S. Abrams, J. P. Dowling, and C. P. Williams, Quantum clock synchronization based on shared prior entanglement, Phys. Rev. Lett. **85**, 2010 (2000).

[33] V. Giovannetti, S. Lloyd, and L. Maccone, Quantum-enhanced positioning and clock synchronization, Nature (London) **412**, 417 (2001).

[34] B. C. Nichol *et al.*, An elementary quantum network of entangled optical atomic clocks, Nature (London) **609**, 689 (2022).

[35] C. Li, T. Li, Y.-X. Liu *et al.*, Effective routing design for remote entanglement generation on quantum networks, npj Quantum Inf. **7**, 10 (2021).

[36] Y. Matsuzaki, S. C. Benjamin, and J. Fitzsimons, Probabilistic growth of large entangled states with low error accumulation, Phys. Rev. Lett. **104**, 050501 (2010).

[37] A. Patil, M. Pant, D. Englund, D. Towsley, and S. Guha, Entanglement generation in a quantum network at distance-independent rate, npj Quantum Inf. **8**, 51 (2022).

[38] M. Pant *et al.*, Routing entanglement in the quantum internet, npj Quantum Inf. **5**, 25 (2019).

[39] P. C. Humphreys, N. Kalb, J. P. J. Morits *et al.*, Deterministic delivery of remote entanglement on a quantum network, Nature (London) **558**, 268 (2018).

[40] N. Kalb, A. A. Reiserer, P. C. Humphreys *et al.*, Entanglement distillation between solid-state quantum network nodes, Science **356**, 928 (2017).

[41] Y. Zhong, H.-S. Chang, A. Bienfait *et al.*, Deterministic multi-qubit entanglement in a quantum network, Nature (London) **590**, 571 (2021).

[42] L. J. Stephenson *et al.*, High-rate, high-fidelity entanglement of qubits across an elementary quantum network, Phys. Rev. Lett. **124**, 110501 (2020).

[43] D. Schlingemann, Cluster states, algorithms and graphs, arXiv:quant-ph/0305170.

[44] M. Hein, J. Eisert, and H. J. Briegel, Multiparty entanglement in graph states, Phys. Rev. A **69**, 062311 (2004).

[45] N. Shettell and D. Markham, Graph states as a resource for quantum metrology, Phys. Rev. Lett. **124**, 110502 (2020).

[46] D. Schlingemann and R. F. Werner, Quantum error-correcting codes associated with graphs, Phys. Rev. A **65**, 012308 (2001).

[47] R. Raussendorf and H. J. Briegel, A one-way quantum computer, Phys. Rev. Lett. **86**, 5188 (2001).

[48] A. H. Shenoy and R. Srikanth, Maximally nonlocal subspaces, J. Phys. A: Math. Theor. **52**, 095302 (2019).

[49] J. C. Adcock, S. Morley-Short, A. Dahlberg *et al.*, Mapping graph state orbits under local complementation, Quantum **4**, 305 (2020).

[50] M. Epping, H. Kampermann, and D. Bruß, Large-scale quantum networks based on graphs, New J. Phys. **18**, 053036 (2016).

[51] A. Pirker and W. Dür, A quantum network stack and protocols for reliable entanglement-based networks, New J. Phys. **21**, 033003 (2019).

[52] M. Cuquet and J. Calsamiglia, Growth of graph states in quantum networks, Phys. Rev. A **86**, 042304 (2012).

[53] F. Hahn, A. Pappa, and J. Eisert, Quantum network routing and local complementation, npj Quantum Inf. **5**, 76 (2019).

[54] A. Pirker, J. Wallnöfer, and W. Dür, Modular architectures for quantum networks, New J. Phys. **20**, 053054 (2018).

[55] E. Schoute, L. Mancinska, T. Islam *et al.*, Shortcuts to quantum network routing, arXiv:1610.05238.

[56] A. W. Marshall, I. Olkin, and B. C. Arnold, *Inequalities: Theory of Majorization and Its Applications* (Springer, New York, 2011).

[57] M. Van den Nest, J. Dehaene, and B. De Moor, Graphical description of the action of local Clifford transformations on graph states, Phys. Rev. A **69**, 022316 (2004).

[58] H. J. Briegel and R. Raussendorf, Persistent entanglement in arrays of interacting particles, Phys. Rev. Lett. **86**, 910 (2001).

[59] de Jong, J., F. Hahn, N. Tcholtchev *et al.*, Extracting maximal entanglement from linear cluster states, arXiv:2211.16758.

[60] F. Hahn, A. Dahlberg, J. Eisert, and A. Pappa, Limitations of nearest-neighbor quantum networks, Phys. Rev. A **106**, L010401 (2022).

[61] D. Leung, J. Oppenheim, and A. Winter, Quantum network communication—the butterfly and beyond, IEEE Trans. Inf. Theory **56**, 3478 (2010).

[62] V. Mannalath and A. Pathak, Entanglement routing and bottlenecks in grid networks, arXiv:2211.12535.

[63] M. A. Nielsen, Conditions for a class of entanglement transformations, Phys. Rev. Lett. **83**, 436 (1999).

[64] G. Gour, M. P. Müller, V. Narasimhachar, R. W. Spekkens, and N. Y. Halpern, The resource theory of informational nonequilibrium in thermodynamics, Phys. Rep. **583**, 1 (2015).

[65] Y. Hasegawa *et al.*, Experimental time-reversed adaptive Bell measurement towards all-photonic quantum repeaters, Nat. Commun. **10**, 378 (2019).

[66] P. Hilaire, E. Barnes, and S. E. Economou, Resource requirements for efficient quantum communication using all-photonic graph states generated from a few matter qubits, Quantum **5**, 397 (2021).

[67] J. de Jong, F. Hahn, J. Eisert, N. Walk, and A. Pappa, Anonymous conference key agreement in linear quantum networks, Quantum **7**, 1117 (2023).